Glycobiology vol. 23 no. 10 pp. 1142–1151, 2013
doi:10.1093/glycob/cwt051
Advance Access publication on July 7, 2013

Deficiency of α-glucosidase I alters glycoprotein glycosylation and lifespan in *Caenorhabditis elegans*

Toshihiko Katoh[2], Juri Takase[3], Yasushi Tani[3], Ryuta Amamoto[3], Naofumi Aoshima[3], Michael Tiemeyer[2], Kenji Yamamoto[4], and Hisashi Ashida[5,1]

[2]Complex Carbohydrate Research Center, The University of Georgia, Athens, GA 30602-4712, USA; [3]Graduate School of Biostudies, Kyoto University, Kyoto 606-8502, Japan; [4]Research Institute for Bioresources and Biotechnology, Ishikawa Prefectural University, Ishikawa 921-8836, Japan; and [5]Faculty of Biology-Oriented Science and Technology, Kinki University, Wakayama 649-6493, Japan

Received on May 15, 2013; revised on June 25, 2013; accepted on June 27, 2013

Endoplasmic reticulum (ER) α-glucosidase I is an enzyme that trims the distal α1,2-linked glucose (Glc) residue from the $Glc_3Man_9GlcNAc_2$ oligosaccharide following its addition to nascent glycoproteins in the initial step of processing. This reaction is critical to the subsequent processing of N-glycans and thus defects in α-glucosidase I gene in human cause congenital disorder of glycosylation (CDG) type IIb. We identified the *Caenorhabditis elegans* α-glucosidase I gene (F13H10.4, designated *agl-1*) that encodes a polypeptide with 36% identity to human α-glucosidase I. The *agl-1* cDNA restored the expression of complex-type N-glycans on the cell surface of α-glucosidase I-defective Chinese hamster ovary Lec23 cells. RNAi knockdown of *agl-1* [*agl-1*(RNAi)] produced worms that were visibly similar to wild-type, but lifespan was reduced to about half of the control. Analyses of *N*-glycosylation in *agl-1*(RNAi) animals by western blotting and mass spectrometry showed reduction of paucimannose and complex-type glycans and dramatic increase of glucosylated oligomannose glycans. In addition, a significant amount of unusual terminally fucosylated N-glycans were found in *agl-1*(RNAi) animals. ER stress response was also provoked, leading to the accumulation of large amounts of triglucosylated free oligosaccharides (FOSs) ($Glc_3Man_{4–5}GlcNAc_{1–2}$) in *agl-1*(RNAi) animals. Acceleration of ER-associated degradation in response to the accumulation of unfolded glycoproteins and insufficient interaction with calnexin/calreticulin in the ER lumen likely accounts for the increase of FOSs. Taken together, these studies in *C. elegans* demonstrate that decreased ER α-glucosidase I affects the entire N-glycan profile and induces chronic ER stress, which may contribute to the pathophysiology of CDG-IIb in humans.

[1]To whom correspondence should be addressed: Tel: +81-736-77-3888; Fax: +81-736-77-4754; e-mail: ashida@waka.kindai.ac.jp

Keywords: Caenorhabditis elegans / congenital disorder of glycosylation / free oligosaccharide / α-glucosidase I / N-glycan

Introduction

N-Glycosylation is one of the major co- and posttranslational modifications of proteins, and plays important roles in protein folding and quality control as well as in conferring stability to the proteins under physiological conditions (Helenius and Aebi 2001). In eukaryotic cells, *N*-glycosylation begins with en bloc transfer of $Glc_3Man_9GlcNAc_2$ moiety from lipid-linked oligosaccharide onto Asn residue of Asn-Xxx-Ser/Thr/Cys sequon (where Xxx is any amino acid except Pro) in the nascent polypeptides by the oligosaccharyltransferase complex in the luminal side of the endoplasmic reticulum (ER) membrane. Most N-linked oligosaccharides are subjected to further processing by the ER/Golgi-resident α-glucosidases and α-mannosidases, and are subsequently converted into hybrid- or complex-type glycans by a variety of glycosyltransferases and modifying enzymes in the Golgi. Although the former part of the glycan-processing pathway is likely common in most eukaryotes, the latter part is diversified widely depending on which species, organs and tissues express any particular glycoprotein.

In the last few decades, many studies have described the importance of *N*-glycosylation, particularly in regard to the early processing pathway's function in protein folding and quality control (Helenius and Aebi 2004). In the initial steps of N-glycan processing, ER α-glucosidase I (mannosyl-oligosaccharide glucosidase or processing α-glucosidase I; EC 3.2.1.106) trims the distal α1,2-linked glucose (Glc) from the $Glc_3Man_9GlcNAc_2$ oligosaccharide after its addition to the nascent protein, and ER α-glucosidase II subsequently removes a α1,3-linked Glc residue, resulting in a monoglucosylated structure ($Glc_1Man_9GlcNAc_2$). This structure is recognized by the ER chaperone proteins calnexin/calreticulin for proper folding of the polypeptide in concert with the co-chaperone oxidoreductase ERp57 (Zapun et al. 1998). A Glc residue on the monoglucosylated structure is then removed by ER α-glucosidase II to release the protein from calnexin/calreticulin for further glycan processing. However, re-glucosylation occurs on the glycans of improperly folded glycoproteins by UDP-Glc:glycoprotein glucosyltransferase, allowing the incompletely folded protein to re-interact with calnexin/calreticulin (Sousa et al. 1992). Proteins that are not productively folded are eventually eliminated from this calnexin/calreticulin cycle and their glycans are trimmed by ER α-mannosidase I and EDEM1/2/3, thereby exposing α1,6-linked Man residue on the C-branch,

which is in turn recognized by ER-lectins such as OS-9 (Clerc et al. 2009; Hosokawa et al. 2010). This leads to the retro-translocation and disposal of the unfolded protein by the ER-associated degradation (ERAD) process (Ruddock and Molinari 2006; Maattanen et al. 2010; Xie and Ng 2010). Thus, a number of glycan-interacting proteins participate in the protein quality control machinery and each glycan structure has significant physiological meaning. Therefore, defects in proper glycan processing could lead to accumulation of immature unfolded glycoproteins in the ER, thereby activating an ER-to-nucleus signaling cascade collectively termed the unfolded protein response (UPR) to relieve this ER stress (Cox and Walter 1996; Sidrauski et al. 1996; Mori 2000). During ERAD, the glycans on unfolded proteins are released by peptide:*N*-glycanase (PNGase) and are subsequently degraded by endo-β-*N*-acetylglucosaminidase (ENGase) in the cytosol (Kato, Kitamura et al. 2007; Suzuki 2007; Chantret and Moore 2008). These free oligosaccharides (FOSs) in the cytosol are transported to the lysosome where they are degraded into monosaccharides.

Decreased ER α-glucosidase I activity in humans causes a severe congenital disorder of glycosylation (CDG) type IIb, which is characterized by dysmorphism, seizures, hepatomegaly, hepatic fibrosis and death at 2.5 months (De Praeter et al. 2000). In CDG-IIb patients, the abundance of unprocessed glucosylated high-mannose (Man) N-glycan structures was increased on glycoproteins and free Glc_3Man_1 oligosaccharides produced by the action of endo-α1,2-mannosidase were detected in urine (De Praeter et al. 2000; Volker et al. 2002). Similar glycan-processing defects were obtained by using α-glucosidase I-deficient Lec23 Chinese hamster ovary (CHO) cells (Ray et al. 1991; Hong et al. 2004) and by treating mammalian cells with α-glucosidase inhibitors (Durrant and Moore 2002; Mellor et al. 2004). Additionally, accumulation of glucosylated FOSs in the cytosol has been reported in these cells (Durrant and Moore 2002; Mellor et al. 2004; Alonzi et al. 2008), which is a characteristic feature of ER α-glucosidase I deficiency.

Caenorhabditis elegans is a suitable model organism for studying N-glycan processing and associated cellular events because its N-glycan structures have been characterized (Cipollo et al. 2002; Natsuka et al. 2002; Haslam and Dell 2003; Hanneman et al. 2006). Also, our previous study expanded the value of this organism in glycobiology by characterizing the FOS structures of *C. elegans* (Kato, Kitamura et al. 2007). Here, we identify the *C. elegans* ER α-glucosidase I gene (designated *agl-1*). Knockdown of *agl-1* by RNAi results in increased unprocessed N-glycans, up-regulation of ER stress response and accumulation of glucosylated FOSs. We also detected and characterized unusual fucosylated structures on glycoproteins in the *agl-1* knockdown worms.

Results

Identification of the gene encoding ER α-glucosidase I in C. elegans

To identify the ER α-glucosidase I in *C. elegans*, we searched the genomic database using human ER α-glucosidase I (hGCS1) as a query (Kalz-Fuller et al. 1995). We found a protein encoded by the gene F13H10.4 showing 36% identity in amino acid sequence with hGCS1. The protein is predicted to be a type II transmembrane protein with a large C-terminal region containing a glycoside hydrolase family 63 domain, which should be oriented into the ER lumen. We amplified the cDNA by reverse transcription-polymerase chain reaction (RT-PCR) using mRNA from *C. elegans* as a template and sequenced the resulting product. The cDNA encodes 799 amino acid residues and is a hybrid form of F13H10.4a and c isoforms reported in WormBase (http://www.wormbase.org/, last accessed 20 June 2013), namely the first exon of F13H10.4a consisting of a 5′-untranslated region connected to F13H10.4c. The amino acid residues whose substitutions lead to reduction of ER α-glucosidase I activity in mammals are conserved in F13H10.4 (Supplementary data, Figure S1). We transiently transfected CHO Lec23 cells, which are defective in ER α-glucosidase I, with the cloned F13H10.4 cDNA and analyzed the surface expression of complex N-glycans using fluorescein isothiocyanate (FITC)-labeled L-phytohaemagglutinin

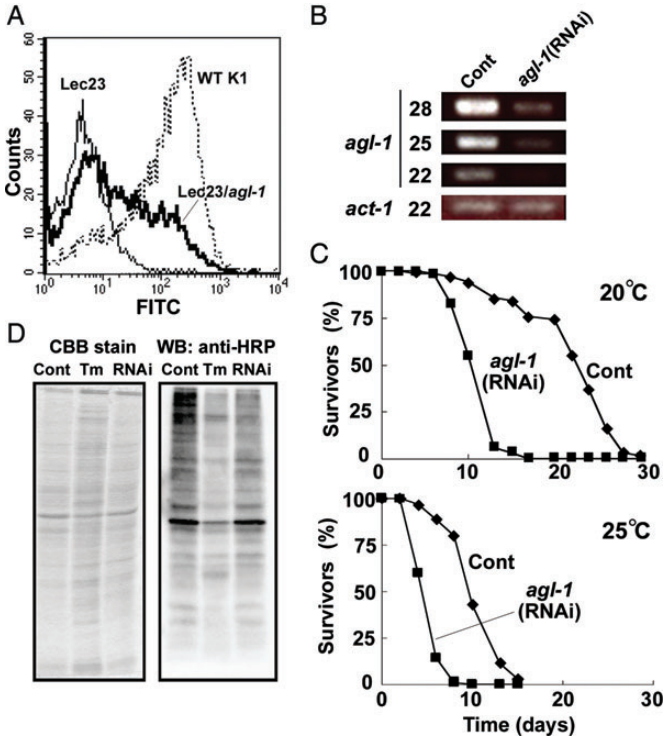

Fig. 1. Knockdown of *agl-1* in *C. elegans*. (**A**) AGL-1 encodes the functional homolog of mammalian ER α-glucosidase I. CHO Lec23 cells were transiently transfected with pME/*agl-1* and then analyzed by FACS using FITC-labeled L-PHA. Thin line, CHO Lec23 cells transfected with mock vector; bold line, CHO Lec23 cells transfected with pME/*agl-1*; dotted line, CHO K1 cells (wild-type). (**B**) Knockdown of *agl-1* by feeding RNAi. Semi-quantitative RT-PCR was performed on *agl-1*(RNAi) and mock-treated worms. The numbers of PCR cycles are shown at left of the panels. The *act-1* transcript was used as a control. (**C**) Lifespan of *agl-1*(RNAi) worms. Roughly synchronized wild-type worms (70 animals per each test) were cultured on *agl-1*(RNAi) (square) or mock control (diamond) plates at 20°C (upper panel) or 25°C (bottom panel). Dead worms were counted every other day. (**D**) Reduction of the core α1,3-linked Fuc in N-glycans of glycoproteins in *agl-1*(RNAi) worms. The same amount of total cell lysate from *agl-1*(RNAi), mock control or TM treated worms was applied onto each lane of SDS–PAGE and proteins were detected by CBB staining (left panel) or western blotting using anti-HRP antibody for α1,3-linked Fuc (right panel).

(PHA) lectin (Figure 1A). F13H10.4 cDNA partially restored the expression of complex N-glycans in CHO Lec23 cells, suggesting that this gene is a functional homolog of mammalian ER α-glucosidase I. Therefore, we named F13H10.4 gene *agl-1* (alpha-glucosidase I).

Knockdown of agl-1 *in* C. elegans *by RNAi*

To investigate the consequence of reduced *agl-1* in *C. elegans*, we knocked down the gene by feeding RNAi. Wild-type worms were fed *Escherichia coli* expressing double-stranded RNA of *agl-1*. The expression level of *agl-1* gene in RNAi knockdown of *agl-1* [*agl-1*(RNAi)] worms was compared with that in mock control by semi-quantitative RT-PCR, and was found to be reduced to less than ~10% of the control (Figure 1B).

We continuously fed wild-type worms with *E. coli* expressing the RNAi construct but observed no visible morphological phenotype and detected no significant differences in the number of laid eggs and hatching rates. However, *agl-1*(RNAi) lifespan was shortened to less than half of the mock control and the relative difference between the populations was maintained at both 20 and 25°C (Figure 1C).

Effect of agl-1 *knockdown on* N-*glycosylation*

Since ER α-glucosidase I is an essential processing enzyme in the *N*-glycosylation pathway, knockdown of *agl-1* gene is anticipated to directly impact on the N-glycome of the organism. Worm N-glycans have been previously characterized by several groups (Altmann et al. 2001; Cipollo et al. 2002, 2005; Natsuka et al. 2002; Haslam and Dell 2003; Paschinger et al. 2004; Hanneman et al. 2006; Schachter 2009) and comprise six groups based on structural characteristics: Oligomannosidic, paucimannosidic, truncated complex, fucose (Fuc)-rich, phosphorylcholine (PC)-rich and core chitobiose modified glycans (Paschinger et al. 2008). In order to evaluate the effect of *agl-1* knockdown on N-glycans, we first performed western blotting using antihorseradish peroxidase (HRP) antibody, which recognizes mature-type core α1,3-fucosylated N-glycans (Paschinger et al. 2004, 2009). As expected, tunicamycin (TM) treatment greatly reduced the reactivity of anti-HRP antibody toward total glycoproteins. The reactivity of glycoproteins harvested from *agl-1*(RNAi) worms was also reduced in comparison with control worms, although the reduction was less than what was detected following TM treatment; the result is nevertheless still compatible with *agl-1*(RNAi) having an effect on N-glycan processing (Figure 1D).

N-Glycosylation changes in *agl-1*(RNAi) worms were further investigated by mass spectrometry (MS). N-Glycans were released from wild-type and *agl-1*(RNAi) glycoproteins by hydrazinolysis because it releases glycans with core chitobiose modifications (e.g. hexose (Hex) extension on the core α1,3-linked Fuc) that could be resistant to digestion by PNGase-F and -A (Hanneman et al. 2006). The released glycans were permethylated and analyzed by nanospray-ionization (NSI)-MS^n using an LTQ/Orbitrap mass spectrometer. We assigned 36 molecular ions corresponding to oligomannosidic, paucimannosidic, truncated complex and Fuc-rich N-glycans from control and *agl-1*(RNAi) worms, but PC-rich glycans were not detected presumably due to loss of those during the permethylation protocol (Figure 2 and Supplementary data, Table S1). In the full MS profile of *agl-1*(RNAi) worms, relative abundances of molecular ions at *m/z* 1312, 1414 and 1516, which correspond to the masses of doubly charged ions of sodium adducts of $Hex_{10}HexNAc_2$, $Hex_{11}HexNAc_2$ and $Hex_{12}HexNAc_2$, respectively, were dramatically increased in comparison with those from control worms. These structures were annotated to be glucosylated oligomannosidic glycans ($Glc_{1-3}Man_{7-9}GlcNAc_2$) based on the Hex content predicted by their compositional mass. These glucosylated oligomannosidic glycans accounted for up to 51% of the total profile in *agl-1*(RNAi) worms, but only 3.4% of the total profile in control worms. In contrast, the relative amounts of further trimmed oligomannosidic ($Hex_{5-9}HexNAc_2$), paucimannosidic and core fucosylated ($Hex_{3-4}HexNAc_2$, $dHex_1Hex_{3-5}HexNAc_2$ and $dHex_2Hex_{4-5}HexNAc_2$) glycans were significantly decreased in *agl-1*(RNAi) worms. The reduction of $dHex_2Hex_{4-5}HexNAc_2$ glycans is consistent with the reduced anti-HRP antibody reactivity detected by western blotting. These results indicate that knockdown of *agl-1* shifts N-glycan processing away from the production of complex-type structures and toward increased prevalence of glucosylated oligomannosidic forms.

Glycomic analyses detected the accumulation of previously undescribed, oligo-Hex structures modified with a single deoxyhexose (dHex) residue at the nonreducing terminal, $dHex_1Hex_{9-11}HexNAc_2$, in *agl-1*(RNAi) worms (Figure 2 and Supplementary data, Table S1). MS^2 fragmentation at *m/z* 1501 (doubly charged ion of $dHex_1Hex_{11}HexNAc_2$, the most abundant dHex-modified oligo- Hex structure) produced a fragment ion at *m/z* 1362, corresponding to the loss of HexNAc at the reducing end. This loss of a single *N*-acetylhexosamine (HexNAc) from the reducing terminus indicates that the dHex residue was not attached to the core chitobiose structure (Figure 3A). The MS^2 profile at *m/z* 1501 also exhibits the fragment ion *m/z* 1027, corresponding to $dHex_1Hex_4$. Furthermore, the *m/z* 707 MS^3 fragment ion (1501-1027-707) is assigned as the $^{3,5}A$ cross-ring cleavage through the α1,6-linked Man residue of the core structure, which is a diagnostic fragment indicating that the C-branch (the branch of Manα1-6Manα1-6Manβ) is modified with the dHex (Figure 3B) (Ashline et al. 2005). Finally, the MS^3 fragment ion at *m/z* 839 (1501-1027-839) corresponds to the loss of nonreducing terminal dHex (−188). Taken together, MS^n analyses indicate that a dHex is attached to a terminal Hex in the C-branch of glucosylated oligomannosidic structures in *agl-1* (RNAi) worm glycoproteins.

Knockdown of agl-1 *causes upregulation of ER stress response*

Impaired N-glycan processing often inhibits calnexin/calreticulin-dependent protein quality control, resulting in the accumulation of unfolded glycoproteins in the ER and the activation of signaling pathways that induce the UPR. The UPR is characterized by the induced expression of an array of genes that help to attenuate the translation rate, facilitate protein folding and degrade unfolded proteins through ERAD. Heat shock protein 4 (HSP-4), an ER chaperone, is one of the proteins induced by the UPR, and is a marker for ER stress (Calfon et al. 2002). Inhibition of *N*-glycosylation by TM induced the expression of green fluorescence protein (GFP)-tagged HSP-4 (*hsp-4*::*gfp*), detected by fluorescence microscopy and by western blotting (Figure 4A and B). Knockdown of *agl-1* showed a similarly significant induction

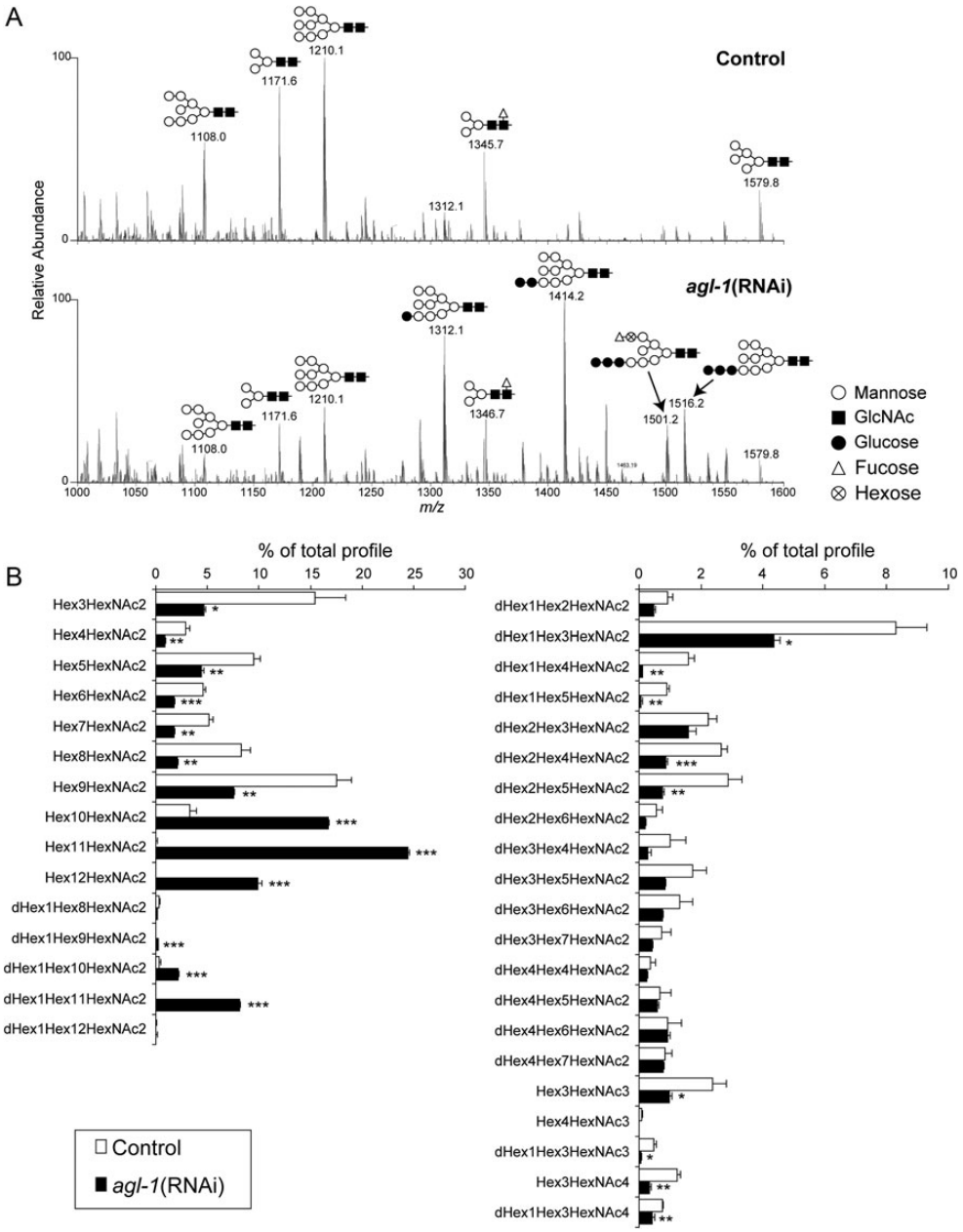

Fig. 2. Analyses of the N-linked glycans from *agl-1*(RNAi) and mock-treated N2 worms. N-Linked glycans were released from glycoproteins by hydrazinolysis, re-*N*-acetylated and permethylated. Permethylated glycans were analyzed using NSI-MS^n (LTQ-Orbitrap). (**A**) Full MS profiles from the control (upper) and *agl-1* (RNAi) (lower) in a range of *m/z* from 1000 to 1600. Major glycan peaks are annotated with the predicted glycan structures. (**B**) Quantification of the prevalence of each N-linked glycan structure. Based on the intensities of glycan signals for each structure, the prevalence of each glycan was quantified as percentage of the total glycan intensity. The averages of three independent experiments with standard errors are shown. Asterisks indicate the significance between control and *agl-1*(RNAi) worms in two-tailed student *t*-test. *$P < 0.05$, **$P < 0.01$ and ***$P < 0.001$.

of HSP-4::GFP (Figure 4A and B), indicating that α-glucosidase I deficiency causes ER stress in *C. elegans*.

Triglucosylated FOSs accumulate in the cytosol of agl-1 *knockdown worms*

Since *agl-1* knockdown strongly induced UPR, ERAD of unfolded glycoproteins should be upregulated. During ERAD, N-linked glycans are cleaved from polypeptides by PNGase and are subsequently processed by ENGase and α-mannosidase in the cytosol (Suzuki et al. 2000, 2006; Blom et al. 2004; Kato, Kawahara et al. 2007; Kato, Kitamura et al. 2007; Chantret and Moore 2008). Unlike mammalian cells, *C. elegans* lacks a cytosolic α-mannosidase (Kato, Kitamura et al. 2007). Therefore, FOSs should retain the nonreducing end structure that the glycoprotein glycan possessed before the unfolded glycoprotein was retro-translocated to the cytosol from the ER. We analyzed FOSs extracted from *agl-1*(RNAi) and mock control by MS. We

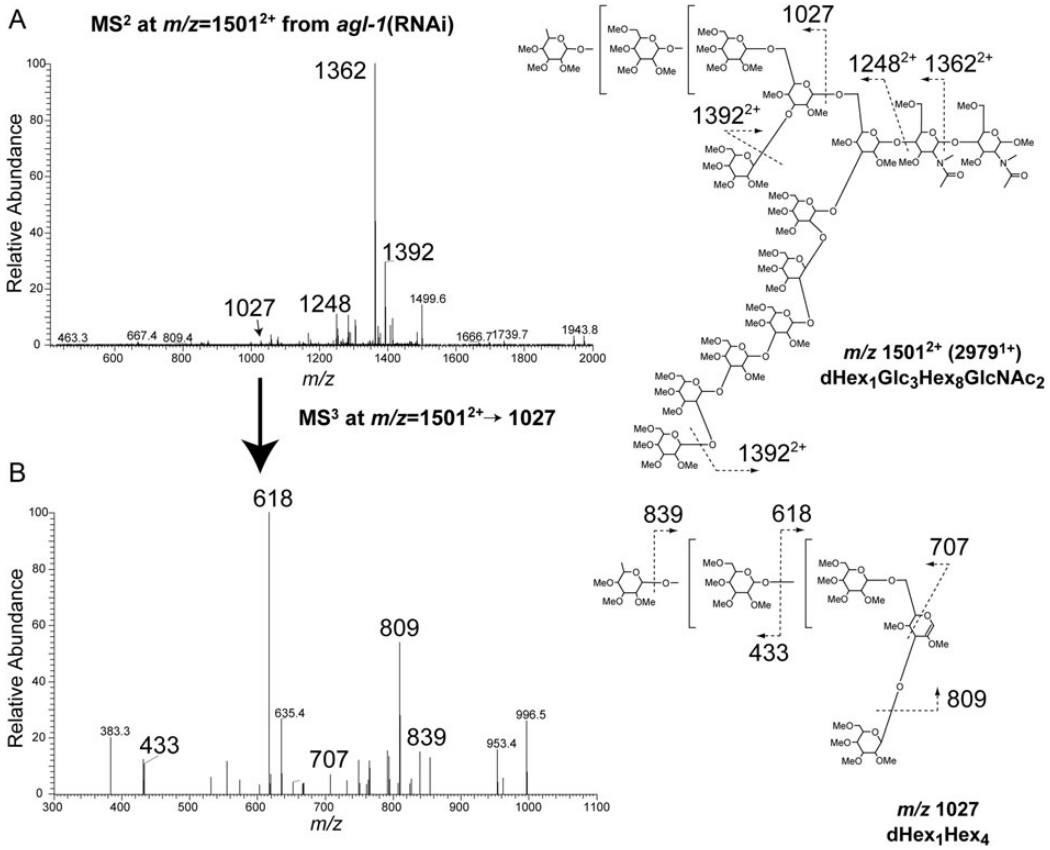

Fig. 3. Fragmentation analysis by NSI-MS^n of a fucosylated, high-mannose glycan of the *agl-1*(RNAi) worms. (**A**) Fragmentation of the permethylated $dHex_1Hex_8HexNAc_2$ at *m/z* 1501^{2+} yields a strong fragment ion at *m/z* 1362^{2+} and a weaker fragment ion at *m/z* 1027 in MS^2. The ion at *m/z* 1362^{2+} corresponds to cleavage between the two GlcNAc residues of the chitobiose core, which indicates that core chitobiose is not fucosylated. The ion at *m/z* 1027 corresponds to fragment of $dHex_1Hex_4$. (**B**) Further fragmentation of ion at *m/z* 1027 yields multiple ions that can be attributed to the Fuc_1Man_4 structure shown at the right. Brackets indicate that the glycan linkages are to be determined.

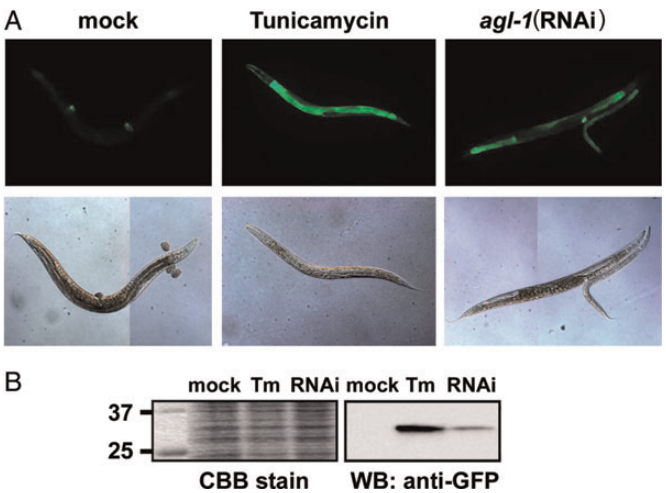

Fig. 4. ER stress induction in *agl-1*(RNAi) worms. L4–adult SJ4005 animals were fed with mock-transfected or *agl-1*(RNAi) expressing *E. coli*, or treated with TM as a positive control. (**A**) Worms were observed by fluorescence microscopy to detect the GFP-tagged HSP-4 reporter protein. Upper panels, GFP fluorescence; lower panels, Nomarski optics. (**B**) Western blotting for GFP-tagged HSP-4. Total proteins were extracted and separated by SDS–PAGE. Proteins were stained with CBB stain or with anti-GFP antibody.

detected a series of molecular ions corresponding to the masses of predicted FOSs in control worms (Figure 5A and Supplementary data, Table S2). Based on peak intensities measured in full MS profiles, the amount of each structure was measured for two sets of FOS species: FOSs with a single GlcNAc (FOS-GN1) and with two GlcNAc (FOS-GN2) at their reducing ends (Figure 5B). FOS-GN2 species are primarily generated by the action of PNGase, and then converted into FOS-GN1 species by the action of ENGase (Kato, Kitamura et al. 2007). In the FOS-GN1 species from the control, short truncated structures ($Hex_{2–3}HexNAc_1$) were relatively abundant, followed by oligomannosidic species, in the order of $Hex_5HexNAc_1$, $Hex_4HexNAc_1$, $Hex_6HexNAc_1$, $Hex_7HexNAc_1$, $Hex_8HexNAc_1$ and $Hex_9HexNAc_1$. In *agl-1*(RNAi) worms, FOS-GN1 species were increased. In particular, $Hex_{7–8}HexNAc_1$ structures were most dramatically increased compared with control.

MS^n analyses were performed to assign the structures of the FOS species that were increased in the *agl-1*(RNAi) worms (Supplementary data, Figures S2 and S3). The MS^2 spectrum of $Hex_7HexNAc_1$ (*m/z* 1742) from *agl-1*(RNAi) gave fragment ions at *m/z* 1261, corresponding to Hex_6 and *m/z* 504, corresponding to $Hex_1HexNAc_1$ (Supplementary data, Figure S2A). The MS^3 spectrum at *m/z* 1465 (1742–1465) also gave the *m/z* 1261 fragment ion (Supplementary data, Figure S2B). The *m/z*

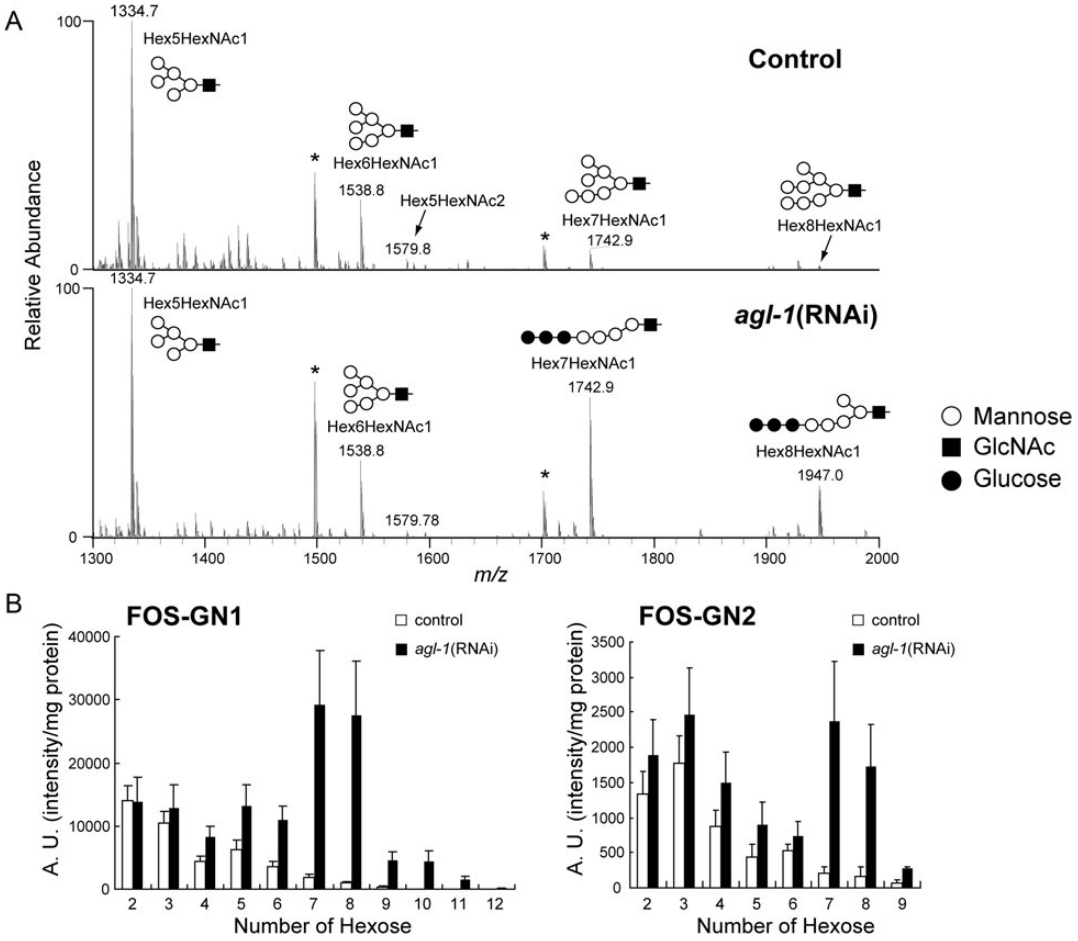

Fig. 5. Analyses of FOSs in *agl-1*(RNAi) and mock-treated worms. FOSs were extracted from *agl-1*(RNAi) and control worms, purified, permethylated and analyzed by NSI-MS^n. (**A**) Full MS profiles of control (upper) and *agl-1*(RNAi) (bottom) worms. Major FOS peaks are annotated with the predicted structures. The annotated structures at *m/z* 1742 and 1946 in *agl-1*(RNAi) reflect the results of MS^n fragmentation analyses (Supplementary data, Figures S1 and S2, respectively). Asterisks indicate contaminant peaks. (**B**) Comparison of the amounts of FOSs with a single GlcNAc residue (FOS-GN1, left panel) and two GlcNAc residues (FOS-GN2, right panel) at their reducing ends for control (open bars) and *agl-1*(RNAi) (filled bars). The amounts of each FOS are shown as arbitrary units (A.U.), defined as peak intensities detected by MS per protein amount (mg) in the extracts. Data are presented as the mean ± standard error for three independent experiments.

1261 fragment ion is produced from linear structure ($Glc_3Man_4GlcNAc_1$) but not from branched, isobaric structures ($Glc_2Man_5GlcNAc_1$ or $Glc_1Man_6GlcNAc_1$/$Man_7GlcNAc_1$, see Supplementary data, Figure S2C). Thus, the structure of the molecular ion at *m/z* 1742 was assigned as the triglucosylated structure, $Glc_3Man_4GlcNAc_1$. Similarly, the MS^2 spectrum of $Hex_8HexNAc_1$ (*m/z* 1947) from *agl-1*(RNAi) gave fragment ions at *m/z* 1261 for Hex_6 and at *m/z* 708 for $Hex_2HexNAc_1$ (Supplementary data, Figure S3). These fragment ions can only be produced from $Glc_3Man_5GlcNAc_1$. Additionally, the $Hex_{7–8}HexNAc_2$ FOSs were markedly increased in *agl-1*(RNAi) worms (Figure 5B) and MS^n analysis revealed that most of these FOS-GN2 species were triglucosylated (data not shown). Thus, knockdown of *agl-1* affects both the N-glycan profile and the FOS profile.

Discussion

The aim of this study was to understand the molecular basis of the consequence of ER α-glucosidase I deficiency. We identified the ER α-glucosidase I gene, *agl-1*, from *C. elegans* and subsequently knocked it down by RNAi. Unexpectedly, *agl-1*(RNAi) worms did not show any visible morphological or behavioral phenotypes, but life span was greatly reduced. To understand the effect of *agl-1* knockdown on the N-linked glycome, we analyzed N-glycan as well as FOS profiles by MS and identified structural changes that are shared in eukaryotic α-glucosidase I-defective cells (Durrant and Moore 2002; Hong et al. 2004; Alonzi et al. 2008). Our glycan profiling took advantage of permethylation to enhance sensitivity and suppress ionization differences between glycan structures, allowing us to obtain relative quantification of glycan changes based on MS signal intensities. The 36 N-glycans that we identified included oligomannosidic, paucimannosidic, truncated complex and Fuc-rich glycans. However, we did not detect PC-rich and native methylated glycans, due to methodological limitation of the permethylation protocol. The predominance of oligomannosidic and paucimannosidic glycans that we detected is in agreement with previous reports (Altmann et al. 2001; Cipollo et al. 2002, 2005; Natsuka et al. 2002; Haslam and Dell 2003;

Paschinger et al. 2004; Hanneman et al. 2006; Schachter 2009). While glucosylated oligomannosidic glycans ($Hex_{10–12}HexNAc_2$) accounted for only 3.4% of the total N-glycan profile in the wild-type control, they increased to more than half of the total N-glycans (51%) in *agl-1*(RNAi). This increase indicates that *agl-1* is critical to N-glycan processing.

Our glycomic analyses also identified a series of terminally dHex-modified (fucosylated) structures ($dHex_1Hex_{9–12}HexNAc_2$) in *agl-1*(RNAi) animals, which accounted for more than 10% of the total N-glycan profile in the knockdown. MS^n analyses revealed that the terminal dHex (Fuc) is attached to a Hex residue of C-branch of the glycan. Previous studies suggested that either Gal (Haslam and Dell 2003) or Man (Cipollo et al. 2002; Hanneman et al. 2006) can be the substrate for the fucosylation, and therefore, determining the Hex species on which fucosylation occurs in *agl-1*(RNAi) is necessary. Similar unusual fucosylation was previously reported in a *C. elegans* triple null mutant lacking UDP-GlcNAc:α-3-D-mannoside β1,2-*N*-acetylglucosaminyltransferase I (GnT-I) (*gly-12*, *-13* and *-14*) as $Fuc_1Hex_{6–9}HexNAc_2$ (Zhu et al. 2004). A shared feature detected both in this triple mutant and in *agl-1*(RNAi) worms is the reduction of native Fuc-rich structures. One possibility for the biological purpose of this unusual fucosylation is that they might be expressed to compensate for the loss of function of the usual Fuc-rich structures. Alternatively, decreased production of the usual Fuc-rich structures may free GDP-Fuc for use by other pathways. Identification and knockdown of the relevant fucosyltransferase(s) will be required in order to assess the functional consequences of these unusual glycans.

Cytosolic FOSs are potentially generated by three different enzymes: Pyrophosphatase acting on dolichol-linked oligosaccharides (Belard et al. 1988), oligosaccharyltransferase (Anumula and Spiro 1983) and PNGase. Among these, PNGase is known to be involved in release of N-glycans from unfolded glycoproteins during ERAD. In yeast *Saccharomyces cerevisiae*, FOSs are undetectable in Δ*png1* cells (Hirayama et al. 2010), indicating that Png1p is the primary enzyme to generate FOSs. We have previously proved that most unfolded proteins were trafficked to the Golgi, based on the observations that M5A FOS-GN1 structure [Manα1-3(Manα1-6)Manα1-6(Manα1-3)Manα1-4GlcNAc] was the most abundant in wild-type and that GnT-1-processed FOS-GN1 structure ($GlcNAc_1Man_5GlcNAc_1$) was abundant in Golgi α-mannosidase II mutant worms. In this study, we detected paucimannosidic FOSs, $Hex_{2–3}HexNAc_1$, as more abundant FOS structures than $Hex_5HexNAc_1$ in wild-type (control). This observation further corroborates the fact that unfolded glycoproteins retain within ER-Golgi compartments because paucimannosidic structures of N-glycan can be made in the Golgi by the action of a series of Golgi enzymes including GnT-I, Golgi α-mannosidase II and processing β-hexosaminidase. This observation also explains why triglucosylated FOSs detected in *agl-1*(RNAi), $Hex_{7–8}HexNAc_{1–2}$, possess a truncated α1,6-Man branch. Thus, most unfolded glycoproteins bearing triglucosylated N-glycans appear to be retained in the Golgi long enough to be acted on by α-mannosidase(s).

In our previous study, we failed to detect paucimannosidic $Hex_{2–3}HexNAc_{1–2}$ glycans as major FOS structures, presumably because of technical limitations of the lectin-capture methodology used in that work (Kato, Kitamura et al. 2007). In this work, we employed an unbiased collection method that was independent of the FOS structure. Therefore, the ratios of FOS species shown in this study are better indicators of the in vivo situation than those reported previously.

Knockdown of *agl-1* caused a reduction of lifespan (Figure 1C). *Caenorhabditis elegans* mutants such as *age-1* (phosphatidylinositol-3-OH kinase) and *daf-2* (insulin-like/IGF-1 receptor) display an extended lifespan with an increased resistance to stress and a reduced metabolic rate (Morris et al. 1996; Kimura et al. 1997; Lin et al. 1997; Ogg et al. 1997). It remains to be determined whether or not the glycan alterations in *agl-1*(RNAi) affects the activity of these previously described lifespan genes. In addition, deficiency of *Mgat1* (GnT-1) gene in *Drosophila melanogaster* produced a severe reduction of lifespan (Sarkar et al. 2006) and, overexpression of GnT-1 in the mutant background not only rescued the shortened lifespan but actually increased lifespan (Sarkar et al. 2010). Therefore, complex glycans appear to play an important regulatory role in determining the lifespan of invertebrates. However, mutants in one or more of the three *C. elegans* GnT-1 genes exhibit variable effects on viability, with the triple null exhibiting extended lifespan under conditions of stress (Zhu et al. 2004). The differing extents of N-glycan processing that occur in various GnT-1 mutant backgrounds may generate unique phenotypes that depend on the specific cell expression patterns for each enzyme. Another report described that RNAi-based knockdown of the worm *mans-1*(D2030.1) that encodes the ortholog of Golgi α-mannosidase IA is associated with a 9% extension in mean lifespan (Liu et al. 2009). Since *agl-1* acts upstream of GnT-1 and Golgi α-mannosidase I, the loss of α-glucosidase activity in affected worm cells results in a global blockage in the production of complex glycans at an earlier step in the N-glycan-processing pathway, thereby producing a greater shift in the glycan profile toward high Man structures. Identifying the glycoproteins that affect lifespan when aberrantly glycosylated will be important for understanding the underlying mechanisms.

ER stress has been shown to trigger autophagy to clear the unfolded proteins from the ER (Bernales et al. 2006; Yorimitsu et al. 2006). We attempted to address whether autophagy was activated by knockdown of *agl-1* by using an autophagy reporter protein, LGG-1::GFP (Melendez et al. 2003). We only detected dots of LGG-1 expression throughout the body of *agl-1*(RNAi) worms and could not detect lipidation of LGG-1 (data not shown). Further experiments will be required to definitively determine whether autophagy contributes to the degradation of unfolded glycoproteins as well as the generation of FOSs in *agl-1*(RNAi) worms. It is known that several types of sugars can trigger autophagy. For example, we have found that the addition of amino sugars such as glucosamine to mammalian cells was able to induce autophagy (Shintani et al. 2010). Also, the natural disaccharide trehalose was reported to be able to induce autophagy and accelerate the clearance of neurotoxic proteins in human cells (Sarkar et al. 2007; Casarejos et al. 2011). In the present study, we demonstrated the accumulation of triglucosylated FOSs in the *agl-1*(RNAi) animals. Generally, in mammalian cells, cytosolic FOSs are cleared from the cytosol by a lysosomal FOS transporter in an ATP-dependent manner. The transport of FOSs into the lysosomes is dependent

on their structures ($Man_3GlcNAc > Man_4GlcNAc > Man_5GlcNAc >> Man_9GlcNAc$); FOS-phosphate are not transported (Saint-Pol et al. 1999). Triglucosylated FOSs were shown to be poor substrates for the lysosomal FOS transporter in HepG2 cells and mouse lymphoma HL60 cells (Moore and Spiro 1994; Mellor et al. 2004). Therefore, glucosylated FOSs is probably not able to gain access into the lysosome through the canonical lysosomal FOS transporter. However, triglucosylated FOSs do not accumulate in the cytosol of CHO Lec23 cells, which lack ER α-glucosidase I, but are cleared from the cells by an as yet undefined mechanism (Durrant and Moore 2002). Although not yet investigated, we predict that autophagy is activated in these cells in response to the presence of glucosylated FOSs, providing an alternative route for elimination of these glycans. Full appreciation of the consequences of ER α-glucosidase I deficiency will require further investigation into whether glucosylated FOSs trigger autophagy in any system. The generation and characterization of the *agl-1*(RNAi) animals reported here provides a platform for future studies.

Materials and methods

Strains and culture of nematode

The N2 Bristol strain was used as the wild-type. Transgenic strain SJ4005, *zcIs4*[*hsp-4::GFP*]*V* (Calfon et al. 2002) was obtained from the *Caenorhabditis* Genetics Center. The strains were maintained at 20°C on nematode growth media (NGM) agar plates with *E. coli* OP50 as a food (Brenner 1974).

Cloning of agl-1 *and construction of plasmids*

Total cDNA was synthesized from total RNA extracted from the wild-type using ReverTra Ace-plus- reverse transcriptase (Toyobo, Japan). The *agl-1* cDNA was amplified by PCR using KOD-plus- DNA polymerase (Toyobo) and the following pair of primers, 5′-CAAGTCGACATGCACAGGGAACATGAAG AG-3′ and 5′-AAAAGCGGCCGCCTAAGTGTCCAAGTTA TCAC-3′. The 2.5 kbp PCR product was digested with *Sal*I and *Not*I, and inserted to pME/FLAG vector to express N-terminally FLAG-tagged AGL-1.

Fluorescence-activated cell sorting

CHO Lec23 cells provided from Prof. P. Stanley were transiently transfected with either pME/FLAG-*agl-1* or mock plasmid, and cultured for 2 days in HAM-12 medium supplemented with 10% fetal calf serum. Cells were harvested and stained with FITC-conjugated L_4PHA lectin (J-Oil Mills, Japan) for 15 min at 4°C, and analyzed by fluorescence-activated cell sorting (FACS) Vantage (BD Bioscience, CA).

Knockdown of agl-1 *by feeding RNA interference*

Feeding RNAi for *agl-1* gene expression in *C. elegans* was carried out as described (Kamath et al. 2000). The *E. coli* HT115 (DE3) harboring RNAi plasmid L4440 or L4440/F13H10.4 (Gene Service, UK) were cultured overnight in Luria-Bertani (LB) medium containing 100 μg/mL ampicillin at 37°C and spotted onto NGM plate supplemented with 25 μg/mL carbenicillin and 1 mM Isopropyl β-D-1-thiogalactopyranoside. L4 worms were transferred onto plates and cultured at 20°C, and the next generation was analyzed. HT115 harboring a mock plasmid L4440 was used for the control. To assess knockdown efficiency, semi-quantitative RT-PCR was performed as follows: Total RNA was extracted with Sepasol RNA I Super (Nacalai Tesque, Japan) from worms frozen in liquid nitrogen and the RNA was then treated with RQ RNase-free DNase (Promega, WI) to digest genomic DNA. Total cDNA was obtained with ReverTra Ace-plus- (Toyobo) and poly dT-primer from the total RNA as template. Using the total cDNA as a template, PCR was performed with Taq polymerase and primer sets, 5′-TAACGAGAAGCACAACGACG-3′ and 5′-GCTTCCGATC CAACAATCAT-3′ for *agl-1*, and 5′-TGTGTGACGACGAGGT TG-3′ and 5′-AGAAGCACTTGCGGTGAACGA-3′ for *act-1*.

Determination of lifespan

Worms were synchronized and young adults were treated with 0.5 mg/mL fluorodeoxyuridine (Sigma-Aldrich, MO) to prevent their progeny from developing. After 24 h, seven worms were transferred to RNAi plates and cultured at 20 or 25°C. Ten plates (total 70 worms) were used for each test.

Western blotting for anti-HRP epitope

Proteins were separated by SDS–PAGE on 12.5% gels and transferred to polyvinylidene fluoride membrane. After blocking with 0.5% bovine serum albumin, membranes were incubated with rabbit anti-HRP (1:12,500, Sigma-Aldrich), and then with HRP-conjugated anti-rabbit IgG (1:2000, Santa Cruz Biotechnology, CA). Detection was carried out using SuperSignal West Pico Chemiluminescent Substrate (Thermo Scientific, IL), followed by development on X-ray films.

Extraction of FOSs from worms

N2 worms fed with bacteria expressing double-stranded RNA of *agl-1* or bacteria harboring control vector on plates were harvested and washed with phosphate-buffered saline. Approximately 100 μL of worms were used for FOS and N-glycan analysis. Worms were homogenized in extraction buffer consisting of 20 mM of HEPES (pH 7.6), 150 mM NaCl, 1 mM EDTA, 1 mM $MgCl_2$, 1 mM $CaCl_2$, complete protein inhibitor cocktail (Roche, Switzerland) on ice. Worm debris and large organelles were removed by spinning down for 10 min at 5000 × *g*. Membrane fractions were further separated by ultracentrifugation (106,000 × *g*, 45 min). One milliliter of cytosolic fraction was used for subsequent analysis. Each protein concentration was assayed with micro BCA protein assay kit (Thermo Scientific). After removing proteins by acetone precipitation, the supernatants were evaporated to dryness. Salts were removed by passing through AG50 resin. FOSs were further purified by using C18 cartridge column (JT Baker, NJ). Pass-through fractions of the C18 column were lyophilized and subjected to derivatization and analysis.

Extraction of glycoproteins from C. elegans *and release of N-glycans*

After separation of cytosol fraction, pellets of worm debris and organelles and of membrane protein fraction were combined. Proteins were precipitated in 80% acetone twice and in 100%

acetone once. They were subsequently denatured by boiling for 5 min and digested with trypsin (Sigma-Aldrich) and chymotrypsin (Sigma-Aldrich) in 0.1 M Tris–HCl (pH8.2), 10 mM $CaCl_2$. The resultant glycopeptides were dried, reconstituted in 5% acetic acid, loaded onto a C18 column preequilibrated with 5% acetic acid. After washing the C18 column with 5% acetic acid, the glycopeptides were eluted by 20% 2-propanol in 5% acetic acid followed by 40% 2-propanol in 5% acetic acid. The eluted glycopeptides were combined and dried. N-Glycans were released by hydrazinolysis followed by re-*N*-acetylation as described previously (Patel et al. 1993). Glycans were purified by passing through a Dowex 50WX8 (H^+ form, Sigma-Aldrich) and C18 column, lyophilized, and subjected to permethylation.

Analysis of glycans by NSI-MS^n

Purified FOSs and N-glycans were permethylated for enhancement of sensitivity and structural determination by MS (Anumula and Taylor 1992). NSI-MS^n analysis of permethylated glycans was performed as previously described (Aoki et al. 2007). Permethylated glycans were dissolved in 1 mM sodium hydroxide in 50% methanol and infused directly into a linear ion trap/orbitrap FT mass spectrometer (LTQ-Orbitrap Discovery, Thermo Scientific) using a nanoelectrospray source at a syringe flow rate of 0.40 µL/min. MS analysis was performed in positive ion mode. For fragmentation by CID in MS/MS and MS^n modes, 35–45% collision energy was applied. The total ion mapping functionality of the Xcalibur software package (version 2.0.7) was performed to obtain MS/MS data for the total glycan profiles. Automated MS and MS/MS spectra were obtained in collection windows that were 2.8 mass units in width. Five scans, each 150 ms in duration, were averaged for each collection window. The *m/z* range from 600 to 2000 was scanned in successive 2.8 mass unit windows with a window-to-window overlap of 0.8 mass units. Glycan prevalence was calculated as % of total profile where the total profile was taken as the sum of the peak intensities for all quantified glycans.

Assays for ER stress induction

For ER stress assay, transgenic worm strain SJ4005 was used. As a positive control for induction of ER stress, SJ4005 was cultured on 2.5 µg/mL TM-containing NGM plates (Calfon et al. 2002). For microscopic analyses, worms were transferred in a drop of 10 mM sodium azide on a 2% agarose pad and fluorescence was observed using a fluorescent microscope (Olympus, Japan) with an exposure time of 0.5 s. Western blotting of tagged GFP was performed with anti-GFP (MBL, Japan) as a primary antibody.

Supplementary data

Supplementary data for this article are available online at http://glycob.oxfordjournals.org/.

Funding

The authors acknowledge the support and access to instrumentation provided through grants from the National Center for Research Resources (P41RR018502) and the National Institute of General Medical Sciences (P41GM103490) from the National Institutes of Health, USA.

Acknowledgements

We thank Drs. Pamela Stanley and Yuko Tashima (Albert Einstein College of Medicine) for providing CHO Lec23 cells, and Dr. Shunji Natsuka (Niigata University, Japan) and Dr. Kazuhiro Aoki (Complex Carbohydrate Research Center, University of Georgia) for valuable discussion.

Conflict of interest

None declared.

Abbreviations

ENGase, endo-β-*N*-acetylglucosaminidase; ER, endoplasmic reticulum; ERAD, ER-associated degradation; FACS, fluorescence-activated cell sorting; FOS, free oligosaccharide; Fuc, fucose, Hex; hexose; HexNAc, *N*-acetylhexosamine; hGCS1, human ER α-glucosidase I; HRP, horseradish peroxidase; HSP, heat shock protein 4; Man, mannose; MS, mass spectrometry; NGM, nematode growth media; NSI, nanospray-ionization; PC, phosphorylcholine; PNGase, peptide:*N*-glycanase; TM, tunicamycin; UPR, unfolded protein response.

References

Alonzi DS, Neville DC, Lachmann RH, Dwek RA, Butters TD. 2008. Glucosylated free oligosaccharides are biomarkers of endoplasmic- reticulum α-glucosidase inhibition. *Biochem J*. 409:571–580.

Altmann F, Fabini G, Ahorn H, Wilson IB. 2001. Genetic model organisms in the study of N-glycans. *Biochimie*. 83:703–712.

Anumula KR, Spiro RG. 1983. Release of glucose-containing polymannose oligosaccharides during glycoprotein biosynthesis. Studies with thyroid microsomal enzymes and slices. *J Biol Chem*. 258:15274–15282.

Anumula KR, Taylor PB. 1992. A comprehensive procedure for preparation of partially methylated alditol acetates from glycoprotein carbohydrates. *Anal Biochem*. 203:101–108.

Aoki K, Perlman M, Lim JM, Cantu R, Wells L, Tiemeyer M. 2007. Dynamic developmental elaboration of N-linked glycan complexity in the *Drosophila melanogaster* embryo. *J Biol Chem*. 282:9127–9142.

Ashline D, Singh S, Hanneman A, Reinhold V. 2005. Congruent strategies for carbohydrate sequencing. 1. Mining structural details by MS^n. *Anal Chem*. 77:6250–6262.

Belard M, Cacan R, Verbert A. 1988. Characterization of an oligosaccharide-pyrophosphodolichol pyrophosphatase activity in yeast. *Biochem J*. 255:235–242.

Bernales S, McDonald KL, Walter P. 2006. Autophagy counterbalances endoplasmic reticulum expansion during the unfolded protein response. *PLoS Biol*. 4:e423.

Blom D, Hirsch C, Stern P, Tortorella D, Ploegh HL. 2004. A glycosylated type I membrane protein becomes cytosolic when peptide: *N*-glycanase is compromised. *EMBO J*. 23:650–658.

Brenner S. 1974. The genetics of *Caenorhabditis elegans*. *Genetics*. 77:71–94.

Calfon M, Zeng H, Urano F, Till JH, Hubbard SR, Harding HP, Clark SG, Ron D. 2002. IRE1 couples endoplasmic reticulum load to secretory capacity by processing the XBP-1 mRNA. *Nature*. 415:92–96.

Casarejos MJ, Solano RM, Gomez A, Perucho J, de Yebenes JG, Mena MA. 2011. The accumulation of neurotoxic proteins, induced by proteasome inhibition, is reverted by trehalose, an enhancer of autophagy, in human neuroblastoma cells. *Neurochem Int*. 58:512–520.

Chantret I, Moore SE. 2008. Free oligosaccharide regulation during mammalian protein *N*-glycosylation. *Glycobiology*. 18:210–224.

Cipollo JF, Awad AM, Costello CE, Hirschberg CB. 2005. *N*-Glycans of *Caenorhabditis elegans* are specific to developmental stages. *J Biol Chem*. 280:26063–26072.

Cipollo JF, Costello CE, Hirschberg CB. 2002. The fine structure of *Caenorhabditis elegans* N-glycans. *J Biol Chem*. 277:49143–49157.

Clerc S, Hirsch C, Oggier DM, Deprez P, Jakob C, Sommer T, Aebi M. 2009. Htm1 protein generates the *N*-glycan signal for glycoprotein degradation in the endoplasmic reticulum. *J Cell Biol*. 184:159–172.

Cox JS, Walter P. 1996. A novel mechanism for regulating activity of a transcription factor that controls the unfolded protein response. *Cell*. 87:391–404.

De Praeter CM, Gerwig GJ, Bause E, Nuytinck LK, Vliegenthart JF, Breuer W, Kamerling JP, Espeel MF, Martin JJ, De Paepe AM, et al. 2000. A novel disorder caused by defective biosynthesis of *N*-linked oligosaccharides due to glucosidase I deficiency. *Am J Hum Genet*. 66:1744–1756.

Durrant C, Moore SE. 2002. Perturbation of free oligosaccharide trafficking in endoplasmic reticulum glucosidase I-deficient and castanospermine-treated cells. *Biochem J*. 365:239–247.

Hanneman AJ, Rosa JC, Ashline D, Reinhold VN. 2006. Isomer and glycomer complexities of core GlcNAcs in *Caenorhabditis elegans*. *Glycobiology*. 16:874–890.

Haslam SM, Dell A. 2003. Hallmarks of *Caenorhabditis elegans* *N*-glycosylation: Complexity and controversy. *Biochimie*. 85:25–32.

Helenius A, Aebi M. 2001. Intracellular functions of *N*-linked glycans. *Science*. 291:2364–2369.

Helenius A, Aebi M. 2004. Roles of *N*-linked glycans in the endoplasmic reticulum. *Annu Rev Biochem*. 73:1019–1049.

Hirayama H, Seino J, Kitajima T, Jigami Y, Suzuki T. 2010. Free oligosaccharides to monitor glycoprotein endoplasmic reticulum-associated degradation in *Saccharomyces cerevisiae*. *J Biol Chem*. 285:12390–12404.

Hong Y, Sundaram S, Shin DJ, Stanley P. 2004. The Lec23 Chinese hamster ovary mutant is a sensitive host for detecting mutations in α-glucosidase I that give rise to congenital disorder of glycosylation IIb (CDG IIb). *J Biol Chem*. 279:49894–49901.

Hosokawa N, Tremblay LO, Sleno B, Kamiya Y, Wada I, Nagata K, Kato K, Herscovics A. 2010. EDEM1 accelerates the trimming of α1,2-linked mannose on the C branch of N-glycans. *Glycobiology*. 20:567–575.

Kalz-Fuller B, Bieberich E, Bause E. 1995. Cloning and expression of glucosidase I from human hippocampus. *Eur J Biochem*. 231:344–351.

Kamath RS, Martinez-Campos M, Zipperlen P, Fraser AG, Ahringer J. 2000. Effectiveness of specific RNA-mediated interference through ingested double-stranded RNA in *Caenorhabditis elegans*. *Genome Biol*. 2:research0002.1–research0002.10.

Kato T, Kawahara A, Ashida H, Yamamoto K. 2007. Unique peptide: *N*-glycanase of *Caenorhabditis elegans* has activity of protein disulphide reductase as well as of deglycosylation. *J Biochem*. 142:175–181.

Kato T, Kitamura K, Maeda M, Kimura Y, Katayama T, Ashida H, Yamamoto K. 2007. Free oligosaccharides in the cytosol of *Caenorhabditis elegans* are generated through endoplasmic reticulum-golgi trafficking. *J Biol Chem*. 282:22080–22088.

Kimura KD, Tissenbaum HA, Liu YX, Ruvkun G. 1997. *daf-2*, an insulin receptor-like gene that regulates longevity and diapause in *Caenorhabditis elegans*. *Science*. 277:942–946.

Lin K, Dorman JB, Rodan A, Kenyon C. 1997. *daf-16*: An HNF-3/forkhead family member that can function to double the life-span of *Caenorhabditis elegans*. *Science*. 278:1319–1322.

Liu YL, Lu WC, Brummel TJ, Yuh CH, Lin PT, Kao TY, Li FY, Liao PC, Benzer S, Wang HD. 2009. Reduced expression of α-1,2-mannosidase I extends lifespan in *Drosophila melanogaster* and *Caenorhabditis elegans*. *Aging Cell*. 8:370–379.

Maattanen P, Gehring K, Bergeron JJ, Thomas DY. 2010. Protein quality control in the ER: The recognition of misfolded proteins. *Semin Cell Dev Biol*. 21:500–511.

Melendez A, Talloczy Z, Seaman M, Eskelinen EL, Hall DH, Levine B. 2003. Autophagy genes are essential for dauer development and life-span extension in *C. elegans*. *Science*. 301:1387–1391.

Mellor HR, Neville DC, Harvey DJ, Platt FM, Dwek RA, Butters TD. 2004. Cellular effects of deoxynojirimycin analogues: Inhibition of *N*-linked oligosaccharide processing and generation of free glucosylated oligosaccharides. *Biochem J*. 381:867–875.

Moore SE, Spiro RG. 1994. Intracellular compartmentalization and degradation of free polymannose oligosaccharides released during glycoprotein biosynthesis. *J Biol Chem*. 269:12715–12721.

Mori K. 2000. Tripartite management of unfolded proteins in the endoplasmic reticulum. *Cell*. 101:451–454.

Morris JZ, Tissenbaum HA, Ruvkun G. 1996. A phosphatidylinositol-3-OH kinase family member regulating longevity and diapause in *Caenorhabditis elegans*. *Nature*. 382:536–539.

Natsuka S, Adachi J, Kawaguchi M, Nakakita S, Hase S, Ichikawa A, Ikura K. 2002. Structural analysis of *N*-linked glycans in *Caenorhabditis elegans*. *J Biochem*. 131:807–813.

Ogg S, Paradis S, Gottlieb S, Patterson GI, Lee L, Tissenbaum HA, Ruvkun G. 1997. The Fork head transcription factor DAF-16 transduces insulin-like metabolic and longevity signals in *C. elegans*. *Nature*. 389:994–999.

Paschinger K, Gutternigg M, Rendic D, Wilson IB. 2008. The *N*-glycosylation pattern of *Caenorhabditis elegans*. *Carbohydr Res*. 343:2041–2049.

Paschinger K, Rendic D, Lochnit G, Jantsch V, Wilson IB. 2004. Molecular basis of anti-horseradish peroxidase staining in *Caenorhabditis elegans*. *J Biol Chem*. 279:49588–49598.

Paschinger K, Rendic D, Wilson IB. 2009. Revealing the anti-HRP epitope in *Drosophila* and *Caenorhabditis*. *Glycoconj J*. 26:385–395.

Patel T, Bruce J, Merry A, Bigge C, Wormald M, Jaques A, Parekh R. 1993. Use of hydrazine to release in intact and unreduced form both N- and O-linked oligosaccharides from glycoproteins. *Biochemistry*. 32:679–693.

Ray MK, Yang J, Sundaram S, Stanley P. 1991. A novel glycosylation phenotype expressed by Lec23, a Chinese hamster ovary mutant deficient in α-glucosidase I. *J Biol Chem*. 266:22818–22825.

Ruddock LW, Molinari M. 2006. N-Glycan processing in ER quality control. *J Cell Sci*. 119:4373–4380.

Saint-Pol A, Codogno P, Moore SE. 1999. Cytosol-to-lysosome transport of free polymannose-type oligosaccharides. Kinetic and specificity studies using rat liver lysosomes. *J Biol Chem*. 274:13547–13555.

Sarkar S, Davies JE, Huang Z, Tunnacliffe A, Rubinsztein DC. 2007. Trehalose, a novel mTOR-independent autophagy enhancer, accelerates the clearance of mutant huntingtin and α-synuclein. *J Biol Chem*. 282:5641–5652.

Sarkar M, Iliadi KG, Leventis PA, Schachter H, Boulianne GL. 2010. Neuronal expression of *Mgat1* rescues the shortened life span of *Drosophila Mgat1* null mutants and increases life span. *Proc Natl Acad Sci USA*. 107:9677–9682.

Sarkar M, Leventis PA, Silvescu CI, Reinhold VN, Schachter H, Boulianne GL. 2006. Null mutations in *Drosophila* *N*-acetylglucosaminyltransferase I produce defects in locomotion and a reduced life span. *J Biol Chem*. 281:12776–12785.

Schachter H. 2009. Paucimannose *N*-glycans in *Caenorhabditis elegans* and *Drosophila melanogaster*. *Carbohydr Res*. 344:1391–1396.

Shintani T, Yamazaki F, Katoh T, Umekawa M, Matahira Y, Hori S, Kakizuka A, Totani K, Yamamoto K, Ashida H. 2010. Glucosamine induces autophagy via an mTOR-independent pathway. *Biochem Bioph Res Commun*. 391:1775–1779.

Sidrauski C, Cox JS, Walter P. 1996. tRNA ligase is required for regulated mRNA splicing in the unfolded protein response. *Cell*. 87:405–413.

Sousa MC, Ferrero-Garcia MA, Parodi AJ. 1992. Recognition of the oligosaccharide and protein moieties of glycoproteins by the UDP-Glc:glycoprotein glucosyltransferase. *Biochemistry*. 31:97–105.

Suzuki T. 2007. Cytoplasmic peptide:*N*-glycanase and catabolic pathway for free *N*-glycans in the cytosol. *Semin Cell Dev Biol*. 18:762–769.

Suzuki T, Hara I, Nakano M, Shigeta M, Nakagawa T, Kondo A, Funakoshi Y, Taniguchi N. 2006. Man2C1, an α-mannosidase, is involved in the trimming of free oligosaccharides in the cytosol. *Biochem J*. 400:33–41.

Suzuki T, Park H, Hollingsworth NM, Sternglanz R, Lennarz WJ. 2000. PNG1, a yeast gene encoding a highly conserved peptide:*N*-glycanase. *J Cell Biol*. 149:1039–1052.

Volker C, De Praeter CM, Hardt B, Breuer W, Kalz-Fuller B, Van Coster RN, Bause E. 2002. Processing of N-linked carbohydrate chains in a patient with glucosidase I deficiency (CDG type IIb). *Glycobiology*. 12:473–483.

Xie W, Ng DT. 2010. ERAD substrate recognition in budding yeast. *Semin Cell Dev Biol*. 21:533–539.

Yorimitsu T, Nair U, Yang Z, Klionsky DJ. 2006. Endoplasmic reticulum stress triggers autophagy. *J Biol Chem*. 281:30299–30304.

Zapun A, Darby NJ, Tessier DC, Michalak M, Bergeron JJ, Thomas DY. 1998. Enhanced catalysis of ribonuclease B folding by the interaction of calnexin or calreticulin with ERp57. *J Biol Chem*. 273:6009–6012.

Zhu S, Hanneman A, Reinhold VN, Spence AM, Schachter H. 2004. *Caenorhabditis elegans* triple null mutant lacking UDP-*N*-acetyl-d-glucosamine:α-3-d-mannoside β1,2-*N*-acetylglucosaminyltransferase I. *Biochem J*. 382:995–1001.